

## Large inverse magnetoresistance in fully epitaxial Fe/Fe<sub>3</sub>O<sub>4</sub>/MgO/Co magnetic tunnel junctions

F. Greullet,<sup>1,a)</sup> E. Snoeck,<sup>2</sup> C. Tiusan,<sup>1</sup> M. Hehn,<sup>1</sup> D. Lacour,<sup>1</sup> O. Lenoble,<sup>1</sup> C. Magen,<sup>2</sup> and L. Calmels<sup>2</sup>

<sup>1</sup>Laboratoire de Physique des Matériaux, Nancy-Université, CNRS, B.P. 239, F-54506 Vandœuvre-lès-Nancy, France

<sup>2</sup>Groupe NanoMatériaux, CEMES-CNRS, 29 Rue Jeanne Marvig, B.P. 4347, 31055 Toulouse, France

(Received 18 October 2007; accepted 15 January 2008; published online 8 February 2008)

Fully epitaxial Fe(001)/Fe<sub>3</sub>O<sub>4</sub>(001)/MgO(001)/Co micron-sized magnetic tunnel junctions have been elaborated on MgO(001) substrates. X-ray reflectivity and high-resolution transmission electron microscopy revealed a good quality and epitaxial growth of the stack with abrupt interfaces. The magnetotransport measurements exhibit a large negative tunneling magnetoresistance (TMR) value for magnetic tunnel junctions including an Fe<sub>3</sub>O<sub>4</sub> layer and a MgO tunnel barrier (−8.5% at 300 K and −22% at 80 K). Moreover, the sign of the TMR changes with the applied bias. We discuss here the structural quality of the samples and the transport measurement results. © 2008 American Institute of Physics. [DOI: 10.1063/1.2841812]

The discovery of a tunneling magnetoresistance (TMR) effect at room temperature (RT) in magnetic tunnel junctions (MTJs) with an amorphous oxide barrier<sup>1,2</sup> has induced intense developments with many possible application prospects (memory devices and sensors). In particular, the role of the electronic structure of the electrodes and the insulating barrier in the electron tunneling process has been at the core of experimental and theoretical efforts in electrode/insulator/electrode systems.<sup>3</sup> The measurement of TMR values above 200% at RT in Fe/MgO/Fe crystalline oxide-based tunnel barriers<sup>4–6</sup> is the result of such intense studies. Because of its high sensitivity to the electronic structure, the tunneling transport has also become an efficient tool to probe the density of states (DOS) of the collecting electrode. Indeed, any change in the DOS induces a specific electrical response of the system. Theoretical calculations performed on Fe<sub>3</sub>O<sub>4</sub> reveal a half-metallic behavior at room temperature with 100% negative spin polarization at the Fermi level.<sup>7–9</sup> Not to mention its high Curie temperature ( $T_C=850$  K), this material is particularly interesting to integrate into heterostructures such as MTJs because of its potentiality to exhibit large TMR values. However, at this stage, the properties of Fe<sub>3</sub>O<sub>4</sub> remain controversial and may be linked to either the different growth methods or the Fe<sub>3</sub>O<sub>4</sub> film thickness but with no real agreement between the different groups. For a complete review, see Ref. 17. In this study, epitaxial Fe/Fe<sub>3</sub>O<sub>4</sub>/MgO/Co MTJs were grown. An Fe(001)/Fe<sub>3</sub>O<sub>4</sub>(001) bilayer was chosen as first electrode for its high stability and quality of the Fe<sub>3</sub>O<sub>4</sub> layer grown on Fe(001) buffer.<sup>10</sup> It allows us to reach an Fe<sub>3</sub>O<sub>4</sub> surface topography close to the single-crystalline one. To our knowledge, the reported TMR values for MgO-based MTJs using Fe<sub>3</sub>O<sub>4</sub> electrodes have never exceeded 0.5% at RT.<sup>11,12</sup> Magnetotransport measurements performed on our high structural quality Fe/Fe<sub>3</sub>O<sub>4</sub>/MgO/Co micron-sized MTJs exhibit a large TMR ratio and a specific bias dependence never reported.

The Fe/Fe<sub>3</sub>O<sub>4</sub>/MgO/Co films were epitaxially grown on MgO(001) substrates by sputtering in an UHV chamber whose base pressure is 10<sup>−8</sup> Torr. The Fe layer was deposited at RT using a magnetron system. The Fe<sub>3</sub>O<sub>4</sub> was grown at 400 °C with a radio frequency power under a 5 × 10<sup>−3</sup> Torr Ar plasma pressure starting from Fe<sub>2</sub>O<sub>3</sub> facing targets which is reduced in the plasma. Then, MgO was grown at 100 °C and Co at RT. A Au capping layer was then deposited to protect the whole stack from oxidation. The flatness of each layer and the epitaxial relationship between them have been checked by *in situ* reflection high energy electron diffraction.

We have elaborated different samples regarding the thicknesses of the layers. Structural investigations performed using x-ray reflectivity (XRR) and high-resolution transmission electron microscopy (HRTEM) reveal no evidence of any change in the structural quality of the multilayer whatever the layer thicknesses are.

The cross-sectional specimens for TEM studies were cut along the (100)MgO planes, glued face to face, then thinned by mechanical grinding and ion milling to the electron transparency. The structures of the different layers and interfaces were investigated by TEM both in conventional and in high-resolution mode using a FEI-F20 microscope fitted with a spherical aberration corrector whose point resolution is 0.13 nm.

Figure 1(a) shows a low magnification TEM bright field image of the multilayer. The insulating barrier appears to be continuous over a long distance. A HRTEM micrograph of the stacking is reported in Fig. 1(b) together with its corresponding Fourier transform from [Fig. 1(c)]. Both clearly evidence the good quality of the epitaxial growth separated by reasonably flat interfaces. Table I gathers the lattice parameters and effective misfits (roughly not exceeding 3%) between the neighboring relaxed layers. Co<sub>1</sub> and Co<sub>2</sub> notations depict the occurrence of two variants in the hcp Co layer, i.e., the hexagonal axis lying parallel to the interface plane and being parallel to the [100] or [010] direction of MgO. This behavior has already been shown in previous studies.<sup>13,14</sup> The two variants for the total epitaxial relation-

<sup>a)</sup>Electronic mail: fanny.greullet@lpm.u-nancy.fr.

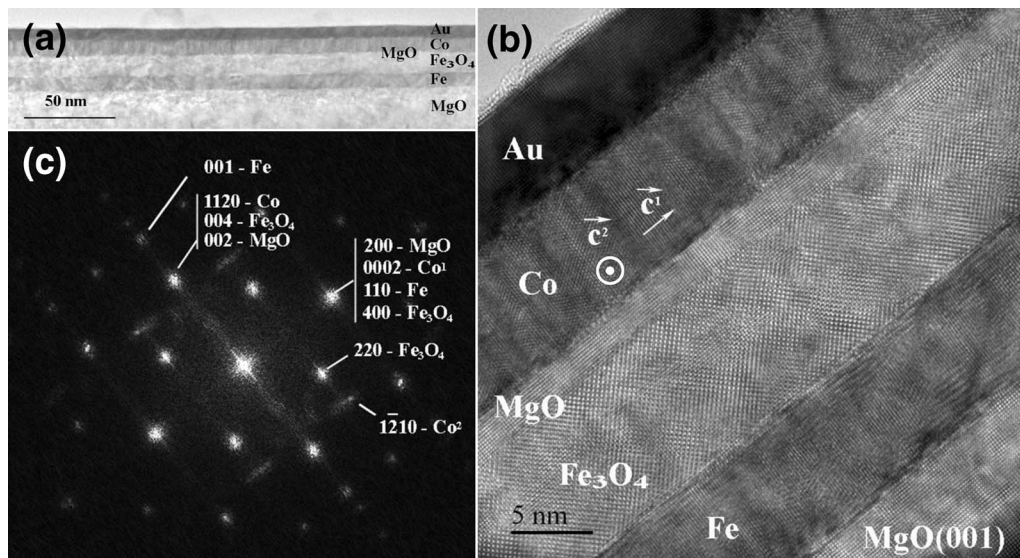


FIG. 1. (a) Low magnification TEM bright field image of MgO(001)/Fe/Fe<sub>3</sub>O<sub>4</sub>/MgO/Co/Au. (b) HRTEM image of the same stacking. (c) Fourier transform of the (b) HRTEM image.

ship are, therefore, MgO-substrate(001)[100]||Fe(001) × [110]||Fe<sub>3</sub>O<sub>4</sub>(001)[100]||MgO(001)[100]||Co<sub>1</sub>(11-20) × [0001] and Co<sub>2</sub>(11-20)[1-100].

A Seifert  $\theta$ -2 $\theta$  x-ray diffractometer fitted with a double monochromator using the Cu K $\alpha$  radiation was used for XRR measurements. The experimental reflectivity profiles were simulated (Fig. 2) using the commercial software X'PERT REFLECTIVITY from PANalytical. This latter adjusts bulk density, thickness, and roughness of the defined layers. The extracted data are gathered in Table II. This experiment indicates that the interfaces of the whole stack are nearly flat especially at the Fe<sub>3</sub>O<sub>4</sub>/MgO and MgO/Co interfaces (mean roughness of about 0.3 nm). The density and thickness of the layers are in agreement with the expected ones.

The high structural quality of the system brought us to perform magnetotransport measurements on Fe (12 nm)/Fe<sub>3</sub>O<sub>4</sub> (8 nm)/MgO (2 nm)/Co (10 nm) multilayer. Thus, we have patterned the continuous layers into micron-sized square-shaped MTJs using standard UV lithography and ion etching techniques. Investigations were made on about 20 junctions with sizes ranging from 10 × 10 to 40 × 40  $\mu\text{m}^2$  and all have revealed the same behavior. The film thickness of Fe<sub>3</sub>O<sub>4</sub> (<10 nm) was chosen to prevent the Verwey transition<sup>15,16</sup> when cooling the sample.<sup>17</sup> Even if we have observed an increase of the resistance-area product in our MTJs when decreasing the temperature, it only doubles, passing from 64 M $\Omega$   $\mu\text{m}^2$  at 300 K to 128 M $\Omega$   $\mu\text{m}^2$  at 80 K. Thus, this behavior shows that the 8 nm thick Fe<sub>3</sub>O<sub>4</sub>(001) preserves its metallic behavior when it is cooled.

TABLE I. Effective misfits between adjacent layers.

	Crystal direction	Lattice parameter (nm)	Effective misfit
MgO subst.	[200]	0.21	
Fe (bcc)	[110]	0.203	+3.3%
Fe <sub>3</sub> O <sub>4</sub> (fcc)	[400]	0.21	-3.4%
MgO (fcc)	[200]	0.21	<1%
Co <sub>1</sub> (hcp)	[0002]	0.203	+3.3%
Co <sub>2</sub> (hcp)	[1-100]	0.19	+9.5%

Figure 3 shows the TMR versus applied bias for a 10 × 10  $\mu\text{m}^2$  MTJ. As convention, in positive bias, the electrons flow from the Fe/Fe<sub>3</sub>O<sub>4</sub> electrode through the Co counter-electrode.

In negative voltage, the TMR decreases and reaches its maximum value at -0.2 V (-8.5% at 300 K and -22% at 80 K). In positive voltage, one can notice a rapid increase of the TMR and a net change of its sign at 80 K at +0.3 V, this latter being more reserved at 300 K. At +0.6 V, the positive TMR achieves a maximum value (+5%), as shown by the inset in Fig. 3.

Interestingly, our magnetotransport measurements depict an abrupt switching of the Fe/Fe<sub>3</sub>O<sub>4</sub> bilayer at small applied magnetic fields (see insets in Fig. 3). This leads to a flat and enduring plateau of 500 Oe where the Fe<sub>3</sub>O<sub>4</sub> magnetization remains homogeneous. This behavior highlights improved magnetic properties of the Fe<sub>3</sub>O<sub>4</sub> layer. Indeed, the Fe<sub>3</sub>O<sub>4</sub> magnetization has been previously reported to be hard to saturate because of the occurrence of antiphase boundaries (APBs).<sup>17</sup> Therefore, in our samples, we argue a drastic reduction of the APBs because of the abrupt switching of the soft bilayer followed by full saturation leading to a large operating field window.

Understanding the specific bias dependence of the TMR remains difficult. The negative spin polarization of the Fe<sub>3</sub>O<sub>4</sub> (Refs. 7-9) is widely accepted and has been experimentally proved for Fe<sub>3</sub>O<sub>4</sub>(001).<sup>18,19</sup> Bataille *et al.*<sup>20</sup> have also found a

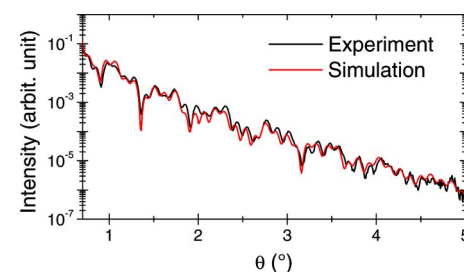


FIG. 2. (Color online) Experimental (black line) and simulated (red line) reflectivity profiles from the XRR measurement of a MgO||Fe/Fe<sub>3</sub>O<sub>4</sub>/MgO/Co/Au multilayer.

TABLE II. Density, thickness, and roughness of the layers extract from the simulation of XRR.

	Bulk density	Simul. density	Simul. thickness (nm)	Simul. roughness (nm)
Fe	7.83	7.75	11.9	0.5
Fe <sub>3</sub> O <sub>4</sub>	5.18	4.76	7	0.25
MgO	3.58	3.27	2	0.3
Co	8.9	8.8	9.9	0.34
Au	19.3	19.3	7.1	0.23

negative spin polarization at Fe<sub>3</sub>O<sub>4</sub>/γ-Al<sub>2</sub>O<sub>3</sub> using spin-resolved photoemission. However, their spin-dependent tunneling experiments in Fe<sub>3</sub>O<sub>4</sub>/γ-Al<sub>2</sub>O<sub>3</sub>/Co MTJ suggest a negative Co tunnel polarization. In our samples, according to the negative TMR, a positive polarization of Co is suggested. Moreover, this polarization changes with applied voltage as shown by the change in sign of the TMR. The influence of the barrier on the spin polarization of the tunneling current has already been highlighted by De Teresa *et al.*<sup>21</sup> In their study, the authors have demonstrated that the barrier can induce a reverse of the tunneling current polarization. Our results show again that the relevant parameter to describe the spin polarized transport in MTJs is the tunneling polarization and not only the electrode polarization. Furthermore, in MgO epitaxial based MTJs, the role of the barrier has already been demonstrated to be symmetry dependent.<sup>6</sup> This makes the analysis of transport using such a simple model impossible. Thus, to have a complete understanding of the observed phenomenon, calculations on the interfacial polarization for both Fe<sub>3</sub>O<sub>4</sub>/MgO and MgO/Co(hcp) are needed.

In conclusion, we have demonstrate the high structural quality of Fe/Fe<sub>3</sub>O<sub>4</sub>/MgO/Co fully epitaxial MTJs grown on MgO(001) substrates. The magnetotransport measurements have revealed a negative TMR value of  $-22\%$  at 80 K with a large and flat plateau of 500 Oe and a change of its sign in positive voltage. The striking behavior of the TMR with applied voltage cannot be understood without calculations on interfacial tunnel polarizations. Moreover, this kind of multilayer could be of great interest in devices applications because of its remaining TMR signal at finite bias.

The authors would like to thank G. Lengaigne for technological process.

<sup>1</sup>J. S. Moodera, L. R. Kinder, T. M. Wong, and R. Meservey, Phys. Rev. Lett. **74**, 3273 (1995).

<sup>2</sup>T. Miyazaki and N. Tezuka, J. Magn. Magn. Mater. **139**, L231 (1995).

<sup>3</sup>W. H. Butler, X. G. Zhang, T. C. Schulthess, and J. M. MacLaren, Phys. Rev. B **63**, 054416 (2001).

<sup>4</sup>S. S. P. Parkin, C. Kaiser, A. Panchula, P. M. Rice, B. Hughes, M. Samant,

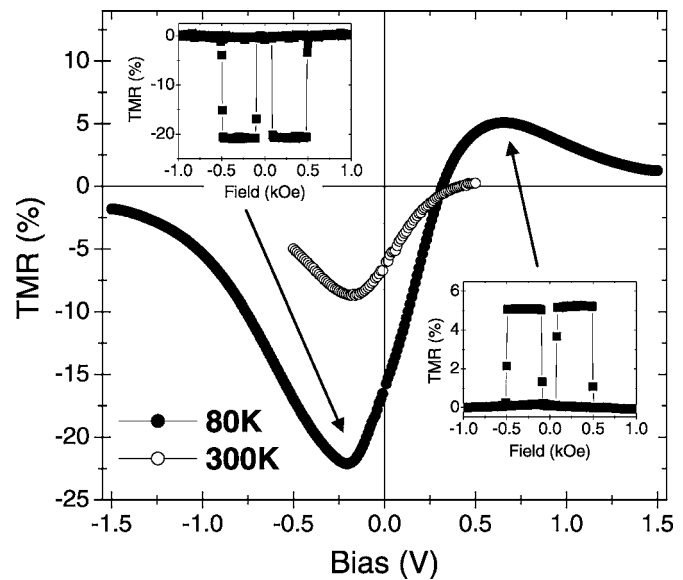


FIG. 3. TMR vs bias curves in Fe/Fe<sub>3</sub>O<sub>4</sub>/MgO/Co MTJs at 300 K (open circles) and 80 K (full circles). Inset: TMR vs field curves at 80 K for  $V = -0.2$  V ( $-22\%$  TMR) and  $V = +0.6$  V ( $+5\%$  TMR).

and S. H. Yang, Nat. Mater. **3**, 862 (2004).

<sup>5</sup>S. Yuasa, T. Nagahama, A. Fukushima, Y. Suzuki, and K. Ando, Nat. Mater. **3**, 868 (2004).

<sup>6</sup>C. Tiusan, F. Greullet, M. Hehn, F. Montaigne, S. Andrieu, and A. Schuhl, J. Phys.: Condens. Matter **19**, 165201 (2007).

<sup>7</sup>A. Yanase and K. Siratori, J. Phys. Soc. Jpn. **52**, 312 (1984).

<sup>8</sup>R. A. de Groot and K. H. J. Buschow, J. Magn. Magn. Mater. **54**, 1377 (1986).

<sup>9</sup>Z. Zhang and S. Satpathy, Phys. Rev. B **44**, 13319 (1991).

<sup>10</sup>N. Spiridis, J. Barbasz, Z. Lodziana, and J. Korecki, Phys. Rev. B **74**, 155423 (2006).

<sup>11</sup>X. W. Li, A. Gupta, G. Xiao, W. Qian, and V. P. Dravid, Appl. Phys. Lett. **73**, 3282 (1998).

<sup>12</sup>P. J. van der Zaag, P. J. H. Bloemen, J. M. Gaines, R. M. Wolf, P. A. A. van der Heijden, R. J. M. van der Veerdonk, and W. J. M. de Jonge, J. Magn. Magn. Mater. **211**, 301 (2000).

<sup>13</sup>H. Wormeester, E. Hüger, and E. Bauer, Phys. Rev. Lett. **77**, 1540 (1996).

<sup>14</sup>J. Faure-Vincent, Ph.D. thesis, Université Henri Poincaré, Nancy, 2004.

<sup>15</sup>E. J. W. Verwey, Nature (London) **144**, 327 (1939).

<sup>16</sup>E. J. W. Verwey, P. W. Haayman, and F. C. Romeijn, J. Chem. Phys. **15**, 181 (1947).

<sup>17</sup>A. M. Bataille, Ph.D. thesis, Université Paris-XI, Orsay, 2005.

<sup>18</sup>D. J. Huang, C. F. Chang, J. Chen, L. H. Tjeng, A. D. Rata, W. P. Wu, S. C. Chung, H. J. Lin, T. Hibma, and C. T. Chen, J. Magn. Magn. Mater. **239**, 261 (2002).

<sup>19</sup>S. A. Morton, G. D. Waddill, S. Kim, I. K. Schuller, S. A. Chambers, and J. G. Tobin, Surf. Sci. **513**, L451 (2002).

<sup>20</sup>A. M. Bataille, R. Mattana, P. Seneor, A. Tagliaferri, S. Gota, K. Bouzehouane, C. Deranlot, M. J. Guittet, J. B. Moussy, C. de Nadaï, N. B. Brookes, F. Petroff, and M. Gautier-Soyer, J. Magn. Magn. Mater. **316**, e963 (2007).

<sup>21</sup>J. M. De Teresa, A. Barthélémy, A. Fert, J. P. Contour, R. Lyonnet, F. Montaigne, P. Seneor, and A. Vaurès, Phys. Rev. Lett. **82**, 4288 (1999).